ARTICLE
Journal of Cellular Biochemistry 108:1211–1219 (2009)

Journal of Cellular Biochemistry

Altered Protein-Expressing Profile in h*PNAS4*-Induced Apoptosis in A549 Human Lung Adenocarcinoma Cells

Lan-Tu Gou, Ai-Ping Tong, Fei Yan, Zhu Yuan, Fei He, Wei Wang, Yan Zhou, Li-Juan Chen, Ming-Hai Tang, and Jin-Liang Yang*

State Key Laboratory of Biotherapy and Cancer Center, West China Hospital, West China Medical School, Sichuan University, Chengdu 610041, Sichuan Province, China

ABSTRACT

Human *PNAS4* (h*PNAS4*) is a recently identified pro-apoptosis gene, which is able to induce apoptosis in A549 human lung adenocarcinoma cells following its overexpression. In this work, we investigated the changes of protein profile in h*PNAS4*-induced apoptosis in A549 cells through proteomic strategy consisting of two-dimensional electrophoresis (2-DE) coupled with MALDI-Q-TOF mass spectrometry. A total of 20 different proteins with more than 3.0-fold change in expression, including 5 up-regulated and 15 down-regulated proteins were successfully identified by database search. The mRNA transcription levels of the different proteins were further examined by RT-PCT. Functional analyses showed these different proteins are involved in diverse biological processes including metabolism, proteolysis, signal transduction, apoptosis, and redox regulation. Two essential apoptosis-associated protein, annexin A1 and prothymosin alpha, were confirmed by Western blot and showed consistent changes with proteomic detection. Our data provide molecular evidence and possible associated pathway in h*PNAS4*-induced apoptosis through proteomic strategy, which should be contributed to further investigation on biological function of h*PNAS4*. J. Cell. Biochem. 108: 1211–1219, 2009.

KEY WORDS: h*PNAS4*; APOPTOSIS; PROTEOMICS; A549 CELL

The gene human *PNAS4* (h*PNAS4*) is a recently identified gene that encodes a 184-amino-acid peptide. Bioinformatics showed the h*PNAS4* sequence is highly homologous to the *PNAS4* of other organisms including mouse, xenopus and zebrafish [MGC Project Team, 2004]. The members of *PNAS4* family share a conserved DUF862 domain with unknown function, suggesting *PNAS4* may play an essential biological role in organic evolution. Recent studies showed h*PNAS4* could be related to certain diseases such as prostate cancer, cervical cancers, and benzene exposure [Best et al., 2005; Forrest et al., 2005; Santin et al., 2005]. By the model organism of zebrafish, we found knocking-down of *PNAS4* causes gastrulation defects with a shorter and broader axis, as well as a posteriorly mis-positioned prechordal plate. Conversely, overexpression of *PNAS4* mRNA leads to an elongated body axis [Yao et al., 2008]. These initial data indicated *PNAS4* should be a key regulator of cell movement in gastrulating. Our recent studies showed h*PNAS4* overexpression could induce apoptosis in A549 human lung adenocarcinoma (A549) cells and suppress tumor growth in mice [Yan et al., 2009]. Therefore, the effective anti-tumor in vitro and vivo show h*PNAS4* is a pro-apoptosis gene that may be used as a potential target of cancer biotherapy. However, the molecular pathway about h*PNAS4* has not been clearly recognized, and it is required to elucidate the related mechanism of apoptosis induced by h*PNAS4*.

Proteomic technologies have been used for identification of proteins associated to molecular mechanism [Dong et al., 2006; Kim et al., 2009]. The global analysis of protein expression complements or has advantage over genomic analyses in certain respects. For instance, proteomic analysis may provide further insight into gene post-translational modifications affecting cellular functions that otherwise could not be detected by genomic analysis [Lee et al., 2004; Zhao and Poh, 2008]. It is generally important to detect changes in global protein expression in order to identify specific proteins participating in apoptosis-related processes [Bruneel et al., 2005; Qiu et al., 2008]. Two-dimensional electrophoresis (2-DE), as the principal tool in proteomics, is able to resolve thousands of proteins in one experiment and present high-resolution in protein separation [Courcelle et al., 2003; Wittmann-Liebold et al., 2006].

Grant sponsor: National Basic Research Program of China; Grant numbers: 2004CB518800, 2004CB518706.

*Correspondence to: Jin-Liang Yang, State Key Laboratory of Biotherapy and Cancer Center, West China Hospital, West China Medical School, Sichuan University, Gaopeng Street, Keyuan Road 4, Chengdu 610041, Sichuan Province, China. E-mail: jlyang01@163.com

Received 22 May 2009; Accepted 21 August 2009 • DOI 10.1002/jcb.22353 • © 2009 Wiley-Liss, Inc.
Published online 30 September 2009 in Wiley InterScience (www.interscience.wiley.com).

The aggregate protein information attainable from such proteomic analyses is able to provide a vast resource for the better understanding of the translated protein milieu and dynamic protein–protein interactions that occur within the intracellular environment in the process of apoptosis. The 2-DE coupled with tandem mass spectrometry (MS/MS) has been used as a rapid and sensitive method to validate the separated proteins, and this powerful tool has been widely applied for investigation on a variety of biological process including cellular apoptosis [Tsai et al., 2005; Chen et al., 2008].

In the present study, we performed overexpression of h*PNAS4* into A549 cells using transient transfection of recombinant plasmid pcDNA3.1(+) and investigated the altered protein expression profile due to the overexpression of h*PNAS4* in A549 cells. We hope proteomics could further reveal the apoptotic mechanism involved in h*PNAS4* and find out essential factor contributing to the apoptosis induced by h*PNAS4*.

MATERIALS AND METHODS

REAGENTS AND ANTIBODIES

The Bio-Rad proteomics platform including chemicals, electrophoresis, and analysis systems was applied in our laboratory. Trypsin Gold™ for protein digestion was purchased from Promega. The reagents related to mass spectrometry were recommended to be chromatographic grade. Mouse antibody against human annexin A1 (ab2487) was purchased from Abcam. Rabbit antibody against human prothymosin alpha (sc-30037) and mouse antibody against human beta-actin (sc-8432) were purchased from Santa Cruz. The secondary antibodies conjugated with horseradish peroxidase against IgG of mouse and rabbit (sc-2005 and sc-2030, respectively) were purchased from Santa Cruz.

PLASMIDS, CELL, AND TRANSFECTION

The recombinant expression plasmid of pcDNA3.1(+) (pc3.1) expressing h*PNAS4* was constructed as previously described [Yan et al., 2009]. Briefly, the open reading frame of h*PNAS4* (GenBank accession: NM_016076) was cloned into plasmid pcDNA3.1(+) (Invitrogen) between *Bam*HI and *Xho*I sites to obtain recombinant plasmids pc3.1-h*PNAS4*. A549 cells (American Type Culture Collection, ATCC) were cultured in Dulbecco's modified Eagle's medium (Gibco) supplemented with 20% fetal bovine serum (Gibco) at 37°C in a humidified incubator with an atmosphere of 5% CO_2. Cells were transiently transfected with pc3.1-h*PNAS4* using Lipofectamine™ 2000 (Invitrogen) according to the manufacturer's instructions for next experiments. PBS, liposome, and pc3.1 were used as controls to assess the effects of h*PNAS4*.

TUNEL ASSAY AND HOECHST STAINING

The cells were seeded in six-well plates at 2.5×10^5 cells per well. Cells were transfected with pc3.1-h*PNAS4*, and then harvested at 48 h post-transfection. For TUNEL assay, approximate 1×10^5 cells in 100 μl PBS were pipetted onto poly-L-lysine-coated glass slides. The cells were fixed by immersing slides in freshly prepared 4% paraformaldehyde solution in PBS for 25 min at 4°C. Apoptotic cells were detected by using DeadEnd™ Fluorometric TUNEL System (Promega) according to the manufacturer's instructions. Hoechst staining (Sigma) was performed according to the manufacturer's instructions, and the morphology of the cell nucleus was observed under a fluorescence microscope (Axiovert 200, Carl Zeiss) at excitation wavelength 350 nm.

TWO-DIMENSIONAL GEL ELECTROPHORESIS AND IMAGE ANALYSIS

About 1×10^7 cells were dissolved in 0.5 ml rehydration buffer (7 M urea, 2 M thiourea, 4% CHAPS, 100 mM dithiothreitol (DTT), 2% ampholyte pH 3–10), and sonicated occasionally with an ultra sonic processor on ice. After short centrifugation, the proteins in supernatant were precipitated with 4 volumes of cold acetone for 30 min at 4°C and subsequently centrifuged at 3,000*g* for 10 min at 4°C. The pellets were resuspended in 400 μl rehydration buffer and centrifuged at 15,000*g* for 30 min at 4°C to remove insoluble fractions. The protein concentration was measured by Protein Assay (Bio-Rad) according to the manufacturer's instructions. For 2-DE, 1 mg of proteins (about 300 μl) was applied to ReadyStrip IPG strip (17 cm, pH 3–10, nonlinear). After 16 h of rehydration at 20°C, the strips were transferred to a PROTEAN IEF Cell. Isoelectric focusing was performed as follows: 250 V, linear, 30 min; 1,000 V, rapid, 1 h; 10,000 V, linear, 5 h; 10,000 V, rapid, 6 h; 500 V, rapid, unlimited time. After isoelectric focusing, the gel strips were equilibrated for 2×15 min in equilibration buffer (25 mM Tris–HCl, pH 8.8, 6 M urea, 20% glycerol, and 2% SDS). DTT (1%) was added to the first equilibration buffer, but replaced by iodoacetamide (2.5%) in the second equilibration buffer. The second dimension electrophoresis was performed with regular 12% SDS–PAGE. The gels were stained in Coomassie Brilliant Blue R-250 Staining Solution and destained in methanol/acetic acid/water (30:10:60, by vol.). The 2-DE was repeated three times to ensure the reliability of results. The gel images were acquired with a scanner (GS-800 Calibrated Densitometer) and subsequently analyzed with PDQuest-7.1 software. Before choosing the differential protein spots, the process of normalization was performed for comparative gels to compensate for nonexpression variation. The ratios of normalized spots intensity in compared gels were calculated basing on PDQuest software analysis, and the spots with more than 3.0-fold difference were selected for subsequent identification by matrix-assisted laser desorption ionization coupled to quadrupole time-of-flight tandem mass spectrometry (MALDI-Q-TOF mass spectrometry, Waters).

IN-GEL DIGESTION

Selected spots were isolated carefully and subjected to in-gel digestion using Trypsin Gold according to the manufacturer's instructions. Briefly, the gel spots were destained twice with 200 μl of 100 mM NH_4HCO_3/50% acetonitrile for 45 min each treatment at 37°C. Then, the destained gel spots were dehydrated in 100 μl of 100% acetonitrile for 5 min at room temperature and subsequently dried in a SpeedVac (Thermo) for 15 min. The dried gel spots were rehydrated with 15 μl of digestion solution (40 mM NH_4HCO_3/10% acetonitrile containing 20 μg/ml trypsin) and digested overnight at 37°C. For extraction of digested peptides, the samples were incubated with 150 μl of deionized water for 10 min with frequent vortex mixing, and the liquid was saved in a new microcentrifuge

tube. The extraction was further performed twice with 50 μl of 50% acetonitrile/5% TFA for 60 min each time at room temperature. Above three extracts were pooled and completely dried in the SpeedVac. Finally, the peptide samples were purified with ZipTip® (Millipore) according to the manufacturer's instructions, eluted in 2 μl of 70% acetonitrile/0.1% TFA containing 10 mg/ml α-cyano-4-hydroxycinnamic acid, and subjected to MALDI-Q-TOF mass spectrometry.

MALDI-Q-TOF MASS SPECTROMETRY ANALYSIS AND DATABASE SEARCH

The peptide samples were analyzed with MALDI-Q-TOF mass spectrometry. The most abundant ions from samples were selected for further analysis of tandem mass spectrometry. The mass spectrometry data were acquired by MassLynx software (Waters) and converted to PKL files that contain mass values and intensity of fragment ions. The PKL files were processed with MASCOT program (www.matrixscience.com). Search parameters were set as follows: Database, Swiss-Prot; taxonomy, *Homo sapiens*; enzyme, trypsin, allowing up to one missed cleavage; peptide mass tolerance, 0.1 Da; MS/MS mass tolerance, 0.01 Da; fixed modification, carbamidomethylation; variable modification, oxidation and phosphorylation. Proteins with probability based MOWSE scores exceeding their threshold ($P < 0.05$) were considered to be positively identified. The functional information of identified proteins was obtained from ExPASy (www.expasy.org/) and NCBI (www.ncbi.nlm.nih.gov.) servers. The isoelectric point/molecular weight (pI/M_w) of identified proteins was calculated by Compute pI/M_w (www.expasy.org/tools/pi_tool.html).

SEMI-QUANTITATIVE RT-PCR

Total RNAs in cells were isolated using Trizol reagent (Invitrogen) according to the manufacturer's instructions. The first-strand cDNA was reversely transcribed from 1 μg RNA in a final volume of 20 μl using RTase and random hexamers from ExScript™ kit (TAKARA) according to the manufacturer's instructions. Primers were designed with Primer Premier 5 software (PREMIER Biosoft International) and searched against GeneBank with NCBI blastn program to ensure sequence specificity. The primer sequence, expected annealing temperature and product length are listed in Table I. The amount of cDNA used for each PCR reaction was 20 ng in a 25 μl reaction volume. PCR was performed with rTaq (TAKARA) in a DNA thermal cycler (Bio-Rad) according to touchdown protocol as follows: 1 cycle of 95°C for 4 min; 10 cycles of 94°C for 45 s, annealing for 45 s (the annealing temperature was set to 5°C above expected annealing temperature with a decrease by 1°C for every cycle), and 72°C for 1 min; 20 additional cycles (shown in preliminary tests to be in linear range) with expected annealing temperature; a final extension at 72°C for 10 min and holding at 4°C. The PCR products were electrophoresed in 1% agarose gel containing a trace of GoldView (SBS Genetech) stain. DNA bands were detected by Gel Doc XR System (Bio-Rad) and analyzed with Quantity One-4.6.1 (Bio-Rad).

WESTERN BLOT

Cells were lysed in RIPA buffer on ice and centrifuged at 15,000 rpm for 1 h at 4°C to obtain the supernatant. The extracted proteins were separated by 12% SDS–PAGE and transferred to PVDF membranes (Amersham Biosciences). The membranes were blocked in 5% skimmed milk for 2 h, and subsequently incubated with primary antibodies for 1 h at room temperature or overnight at 4°C. Then, the membranes were washed with PBST three times and probed by secondary antibodies conjugated with horseradish peroxidase for 1 h at room temperature. After washing the membranes three times with PBST, the immunoblots were visualized with enhanced chemiluminescence system SuperSignal West Pico Chemiluminescent Substrate (Pierce). Three independent experiments were repeated to assess the relative protein levels.

TABLE I. Primers Used in This Study

Gene	Sense (5′→3′)	Anti-sense (5′→3′)	Annealing temperature (°C)	Products size (bp)
VCP	GAGTCCTTGAATGAAGTAGGGTATGAT	GCTGTTGGGTCTGTTGGTTGC	56	471
LMNA	ACGACGAGGATGAGGATGGAGA	GAGGTGAGGAGGACGCAGGAA	58	397
ANXA1	TCTAACTAAGCGAAACAATGCACAG	AAGTCCTCAGATCGGTCACCCT	56	372
MDH2	CCGCCTGACCCTCTATGATATCC	TCCGGCTTTAGCCTTGACCAC	59	577
PRDX6	TCCGTTTCCACGACTTTCTGG	GCTCTTTGGTGAAGACTCCTTTCG	57	564
TPI1	CTCAGAGCACCCGTATCATTTATGG	CCTAGGGAACCCAGGAGCAAA	58	435
EIF4H	CTTCGACACCTACGACGATCG	TTTTCTGAATCCAAAGCCACCT	56	382
BLVRB	TACGAAGTGACAGTGCTGGTGC	AGAGTGCTACTGGTACTGGTGGG	56	546
TAGLN2	TGGCAGTAGCCCGAGATGAT	TGACAGGACAGGCTGAACCC	55	338
NME2	GAACACCTGAAGCAGCACTACATT	CCACCTCTTATTCATAGACCCAHTC	55	331
LGALS1	TTCAACCCTCGCTTCAACGC	GCTGATTTCAGTCAAAGGCCACA	58	280
PTMA	ATTGTTCCTCATCCGCCTCCTTG	CTCGTCGGTCTTCTGCTTCTTGG	61	473
RPLP2	CGACGACCGGCTCAACAA	ATCCCATGTCATCATCTGACTCTT	54	227
SRI	ACATCGCCTGCTGCGTCAA	ATGGCTCAGGAAAGTTCTAAATGGTG	58	354
PSMB6	ATGGCGGGAATCATCATCG	TTCAGGCGGGTGGTAAAGTG	56	337
VIM	TGACCGCTTCGCCAACTACA	CAGCTCCTGGATTTCCTCTTCG	57	403
CALU	AAATAGATGGCGACAAGGACGG	CTTATCCCGAAACTCAACAAACTGC	58	494
RCN1	GACCTTCGACCAGCTCACCC	CGGAATTCGTTAAACTGCTCCC	57	558
EIF3S2	CGGTCTTACTCACGTTGCGGC	CGGACAGCCGAATTGGTCTTG	60	332
LDHB	TCTCCGCACGACTGTTACAGA	CGTAAGAATGTCCACTGGGTTG	54	487
Actin	AGCGGGAAATCGTGCGTGAC	GCCTAGAAGCATTTGCGGTGG	60	517

RESULTS

THE APOPTOSIS INDUCED BY h*PNAS4*

We previously demonstrated overexpression of h*PNAS4* could induce apoptosis in A549 cells. In this work, we further performed TUNEL assay and Hoechst staining to provide evident to confirm the h*PNAS4*-induced apoptosis (Fig. 1A). TUNEL showed there were significantly increased apoptotic cells in h*PNAS4*-treated group compared with PBS and empty vector groups. Morphologically, the comprehensive cell death was observed under light microscope at 48 h after transfection of h*PNAS4*, in which evident chromatin condensation and segregation in h*PNAS4*-transfection cells were visualized by Hoechst staining (Fig. 1B). These results confirm that apoptosis occur following overexpression of h*PNAS4* in A549 cells.

ALTERED PROTEIN PROFILE IN h*PNAS4*–INDUCED APOPTOSIS

Applying 2-DE, we compared protein profiles in A549 cells transfected with pc3.1-h*PNAS4* and empty vector pc3.1, respectively. Approximately 800 protein spots were detected on each gel by PDQuest software, which are localized in the ranges of pI 3–10 and M_r 10–130 kDa (Fig. 2). Before choosing the differential protein spots, the process of normalization in PDQuest was performed for each gel to compensate for nonexpression-related variation. Through PDQuest analysis, change ratios of normalized spots intensities were calculated, and the spots showing more than 3.0-fold difference were selected to be digested and subsequently identified by mass spectrometry (Fig. 4). When searching the database, the proteins whose score exceeded the threshold ($P < 0.05$) were considered to be identified, which indicates identification at 95% confidence level for the matched peptides. A total of 23 spots, including 8 up-regulated and 15 down-regulated spots in h*PNAS4* gel were successfully identified by MALDI-Q-TOF mass spectrometry (Fig. 3). The related information of identified proteins was summarized in Table II. It is noted that malate dehydrogenase and vimentin both have two spots on 2-DE gel, and another protein is h*PNAS4*. Therefore, there were a total of 20 differential proteins that actually come from 23 spots in our study.

TRANSCRIPTION CHANGES OF IDENTIFIED PROTEINS IN h*PNAS4*–INDUCED APOPTOSIS

As far as gene expression is concerned, the change of mRNA transcription level could be considered as an important reason for the change of protein level. Therefore, the investigations on mRNA level can provide better understanding about the mechanism of differential protein expression. To reveal the correlation between the protein levels detected by proteomic analysis and their gene transcription, the mRNA levels of identified proteins were further examined by semi-quantitative RT-PCR (Fig. 4). For the most identified proteins including *LMNA*, *ANXA1*, *PRDX6*, *TPI1*, *BLVRB*, *NME2*, *PTMA*, *RPLP2*, *PSMB6*, *RCN1*, and *LDHB*, their transcriptional mRNA changes were similar to the protein changes on 2-DE gels, which indicates that the overexpression of h*PNAS4* could regulate the expression of these genes at transcription level. Besides, there were eight genes including *MDH2*, *EIF4H*, *TAGLN2*, *LGALS*, *SRI*, *VIM*, *CALU*, and *EIF3S2*, showed no change (less than 2.0-fold change) at mRNA levels, which indicates there could be post-transcription regulation that are responsible for the expression changes of these genes. Interestingly, *VCP* was examined to be up-regulated on 2-DE gel, but its mRNA level was down-regulated, which suggests there is a complicated regulation mechanism that leads to the variance between the protein and mRNA level.

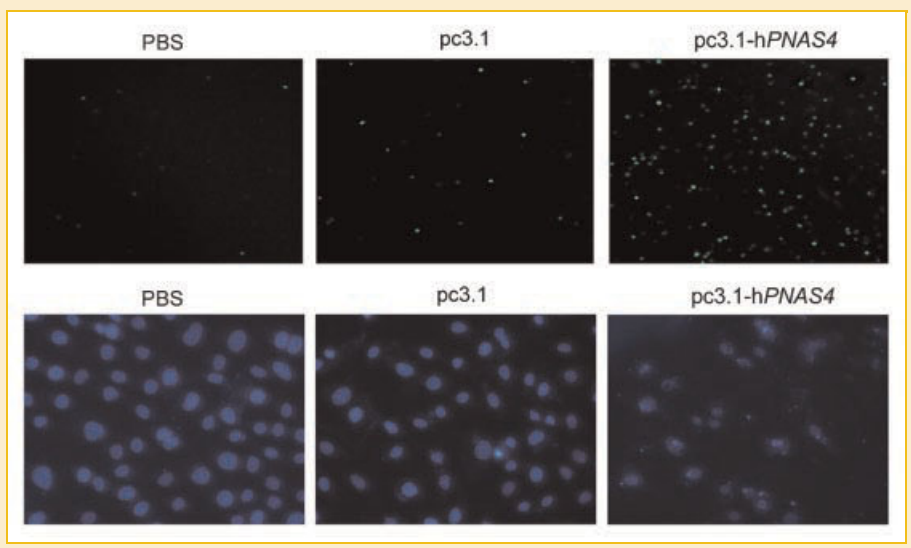

Fig. 1. Cell apoptosis detected by TUNEL assay and Hoechst staining. A549 cells were cultured in chamber slides and allowed to attach for 24 h. Cells were treated with PBS, pc3.1, and pc3.1-h*PNAS4*, respectively, for 48 h. Apoptotic effect was detected by TUNEL assay and viewed under an inverted microscope (100×). TUNEL-positive cells in pc3.1-h*PNAS4* treatment group were significant increased compared with the groups treated with PBS and pc3.1. Hoechst staining (400×) showed evident chromatin condensation and segregation characteristics in h*PNAS4*-overexpressing cells, which were rarely observed in PBS and pc3.1 treated cells. [Color figure can be viewed in the online issue, which is available at www.interscience.wiley.com.]

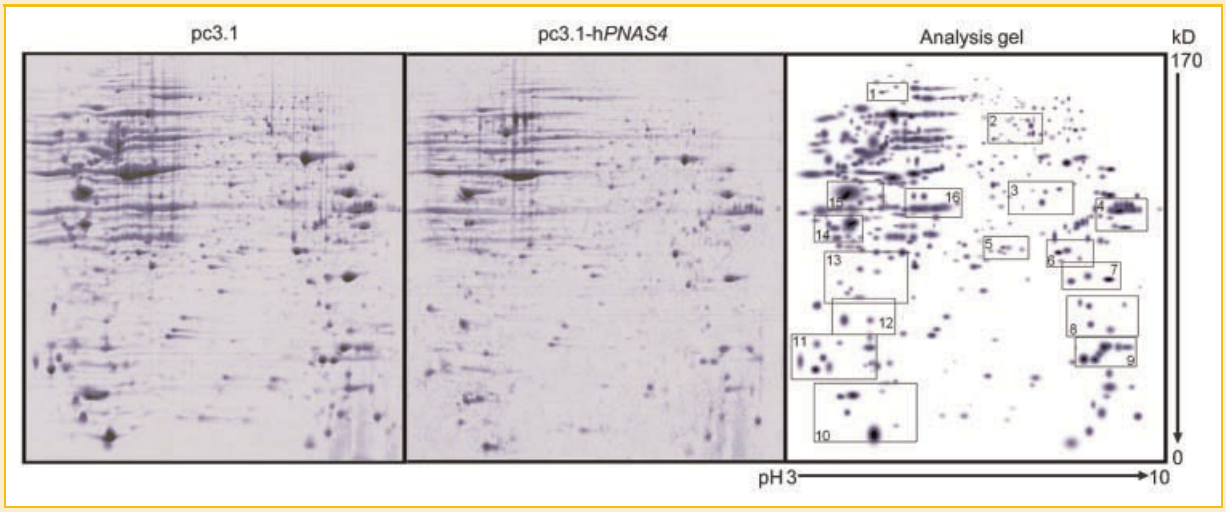

Fig. 2. Representative 2-DE gels of extracted proteins from A549 cells. Cells were treated with pc3.1 and pc3.1-h*PNAS4*, respectively, for 48 h. Total protein extracts (800 μg) were separated on the IPG strip (17 cm, pH 3–10, nonlinear) in the first dimension followed by 12% SDS–PAGE in the second dimension. The gels were visualized by Coomassie Brilliant Blue staining and captured by PDQuest software. The virtual analysis gel was generated by PDQuest for differently comparative analysis. The boxed areas in analysis gel indicate protein spots with at least 3.0-fold expression changes between pc3.1 and pc3.1-h*PNAS4* gels. [Color figure can be viewed in the online issue, which is available at www.interscience.wiley.com.]

VALIDATION OF DOWN-REGULATED PROTHYMOSIN ALPHA AND UP-REGULATED ANNEXIN A1 BY WESTERN BLOT

It is necessary to validate the different protein of interest through Western blot, because there could be more than one spot for certain proteins on 2-DE gel in certain circumstances. These spots actually derive from the same protein and may be generated by post-translational modification such as glycosylation and phosphorylation, which results in the change of mobility on 2-DE gel due to their different isoelectric point and molecular weight. Hence, false results might occur when only concentrating on one spot of those proteins and neglecting other spots changes, because one spot could not represent the total change of the protein. Western blot is an effective tool to reveal the total changes of the proteins with more than one spot on 2-DE gel. Therefore, we further performed Western blot to detect the expression changes of two identified proteins, prothymosin alpha and annexin A1. The major reason why we choose the two proteins is considering their important biological functions involved in cell apoptosis and proliferation. Western blot demonstrated there were down-regulated prothymosin alpha but up-regulated annexin A1 in h*PNAS4*-induced apoptosis of A549 cells, which are consistent with the results from 2-DE (Fig. 5). To a certain extent, the evidence from Western blot reflects the result reliability of the differential proteins detected by 2-DE in this study.

DISCUSSION

Previously, we demonstrated overexpression of h*PNAS4* induces apoptosis in A549 cells [Yan et al., 2009]. In the present study, we applied high-throughput proteomic tools concluding 2-DE and MALDI-Q-TOF mass spectrometry to investigate altered protein-expressing profile in apoptotic A549 cells. Through proteomic comparison between apoptotic and control A549 cells, we hope we may find the proteins involved in apoptosis induced by h*PNAS4* and reveal its potential apoptotic network. And moreover, the obtained information in proteomic aspect will further provide helpful comprehension on biological function of h*PNAS4*.

Consistent with previous studies, our data from TUNEL assay and Hoechst staining demonstrated that overexpression of h*PNAS4* significantly inhibits cell growth and induces apoptosis in A549 cells. Proteomic analysis in this study identified a total of 20 differentially expressed proteins, including 5 up-regulated proteins and 15 down-regulated proteins. These proteins have diverse features and involve in a variety of biological processes such as metabolism, proteolysis, signal transduction, apoptosis, as well as redox regulation. The molecular networks consisting of these identified proteins reflect complicated biological process in apoptosis induced by h*PNAS4*, and provide valuable information to elucidate mechanism of h*PNAS4*-induced apoptosis. It is still necessary to further analyze these differential proteins and reveal their potential interaction to h*PNAS4*, which requires in-depth and detailed investigation in next studies.

Besides proteomic investigation, we further examined the mRNA changes of the 20 differential proteins by RT-PCR. It is interesting that the mRNA levels of eight differential proteins showed no change, and one protein even showed reverse expression change between RT-PCR and 2-DE. In fact, this phenomenon is not incomprehensible in biological experiments [Chen et al., 2002; Ørntoft et al., 2002], and we think there are several reasons as followed corresponding to it. Firstly, post-transcription regulation, an important mechanism of gene expression regulation such as different mRNA translation state [Zong et al., 1999], codon bias [Kurland, 1991], and Kozak rule [Pesole et al., 2000], may lead to the

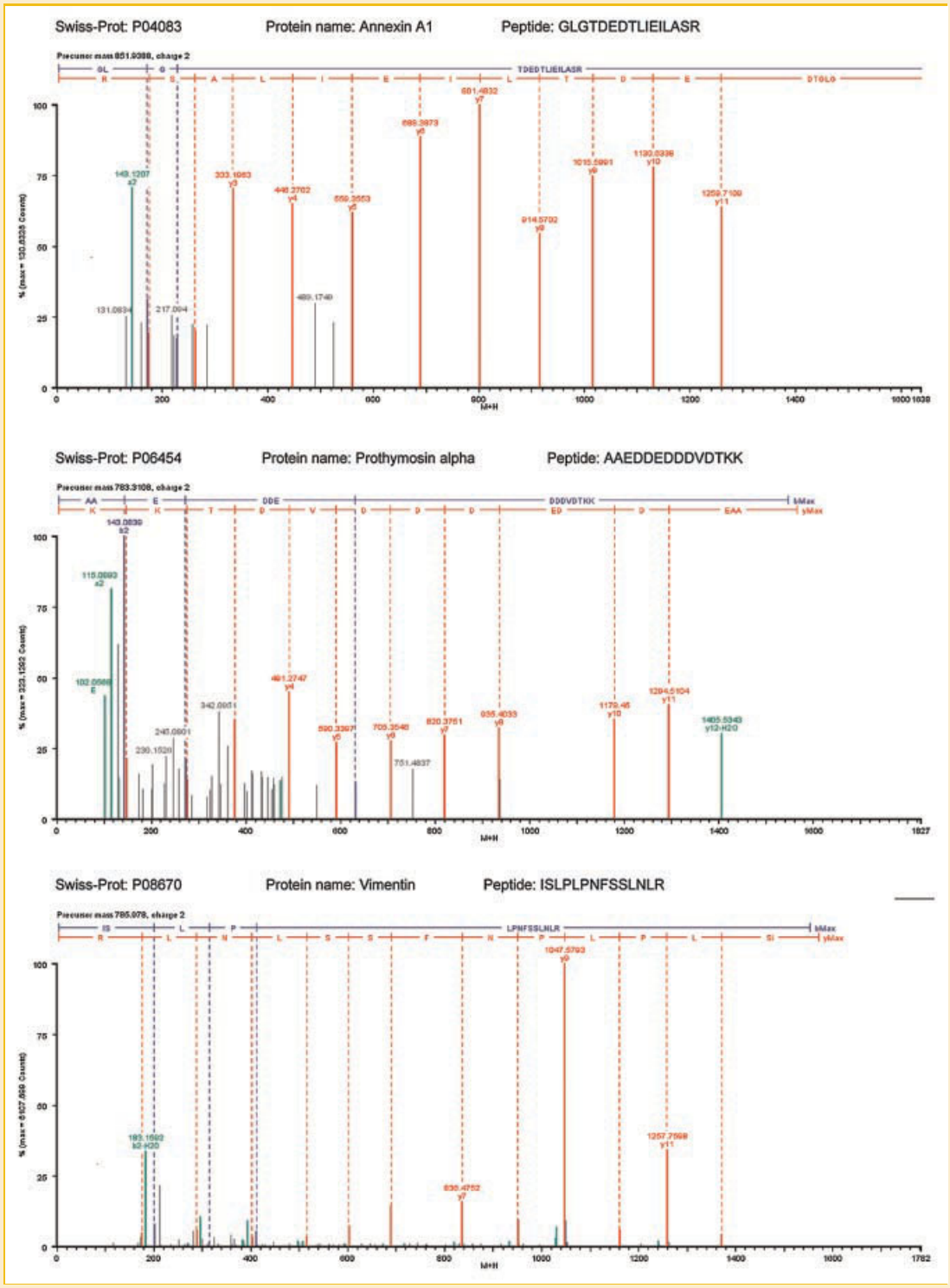

Fig. 3. Representative tandem mass spectrometry maps. Proteins annexin A1 (top), prothymosin alpha (middle), and vimentin (bottom) were successfully identified by MALDI-Q-TOF mass spectrometry. Their Swiss-Prot accession number, protein name, and identified peptide are shown, respectively. [Color figure can be viewed in the online issue, which is available at www.interscience.wiley.com.]

discordant levels of mRNA and protein. Secondly, various half-life of proteins represents protein stability and results in different protein levels [Varshavsky, 2003; Beyer et al., 2004]. Thirdly, amino acid modification such as glycosylation and phosphorylation [Reinders et al., 2004], can cause different mobility in electrophoresis due to their different isoelectric point and molecular weight. Finally, alternative RNA splicing can bring about various transcript variants that encode distinct protein isoforms [Maniatis and Tasic,

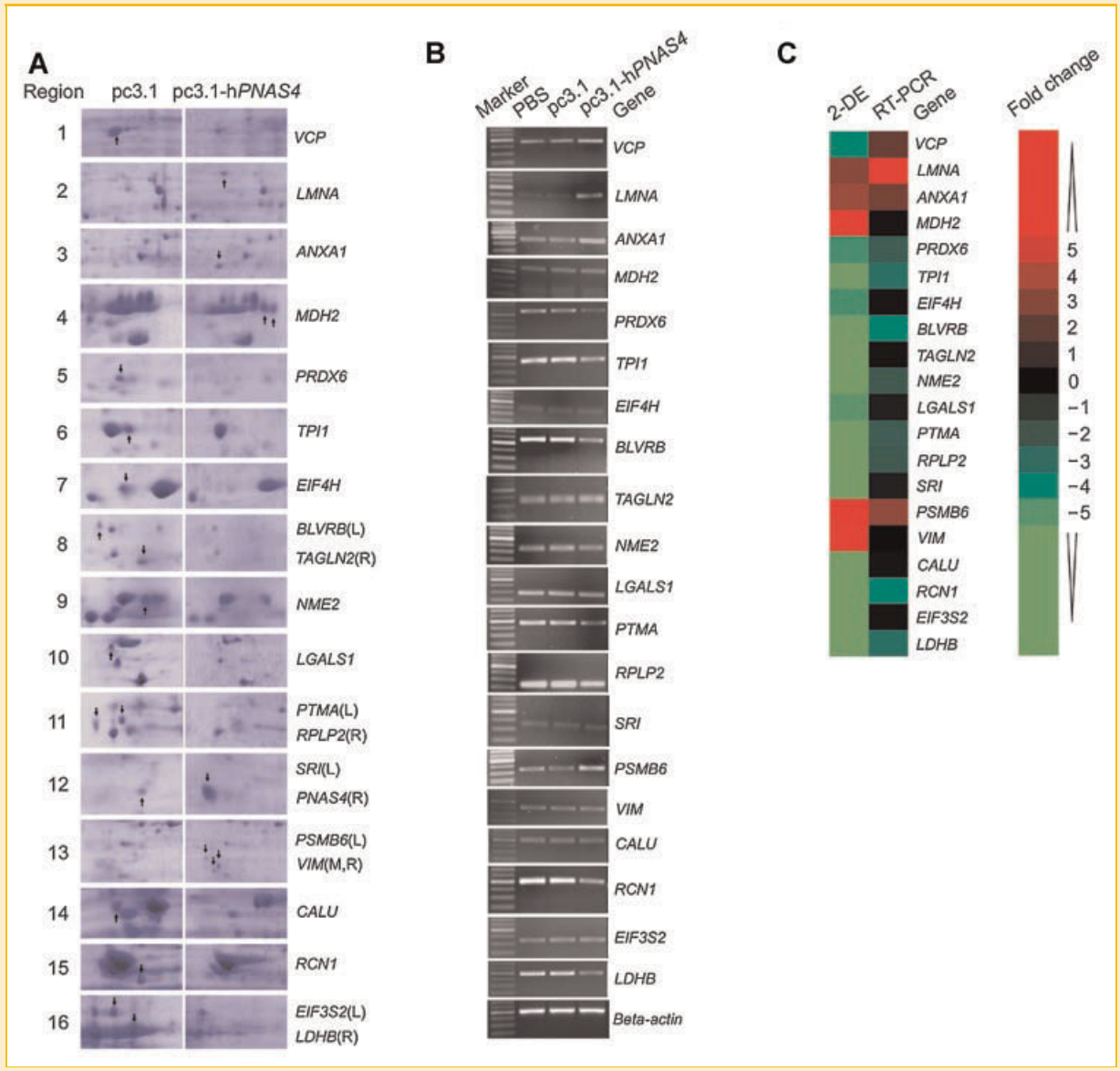

Fig. 4. The illustration of differential proteins on 2-DE gel and mRNA transcription levels. A: The 16 detailed regions on 2-DE gels containing differential proteins are shown. The arrows indicate differential proteins. L, left arrow; M, middle arrow; R, right arrow. B: The mRNA levels of differential proteins were examined by RT-PCR. C: The cluster showing the expression changes of 2-DE and RT-PCR for identified proteins. [Color figure can be viewed in the online issue, which is available at www.interscience.wiley.com.]

2002]. In some instances, post-translational modification and distinct isoforms of proteins may result in biological function deviation, although their mRNA levels remain invariable. Therefore, comprehensive analysis of protein and mRNA levels could more precisely describe the substantial genes expression. And thus, we think our data obtained from RT-PCR further complement expression analysis of the differential proteins and provide instructive comprehension to the results from proteomics.

Among the differential proteins, we are particularly concerned about two apoptosis-related proteins, prothymosin alpha and annexin A1, and their expression changes were further confirmed by immunoblotting to be consistent with the results from 2-DE and RT-PCT. Oncoprotein prothymosin alpha, a highly acidic nuclear protein, can promote cell proliferation through suppression of apoptosome formation to inhibit caspases activation. And, recent studies have demonstrated prothymosin alpha knockdown can lead to Hela cell apoptosis [Jiang et al., 2003; Malicet et al., 2006]. Annexin A1, a member of the calcium-dependent phospholipid binding protein family, represents pro-apoptosis effect through MAPK inhibition, Erk repression, and caspase-3 activation [Debret et al., 2003; Bensalem et al., 2005], indicating annexin A1 may act as a tumor suppressor gene and modulate cell proliferation and apoptosis. Although we have no direct evidence to define the association between h*PNAS4* and the two proteins, we speculate that decreased prothymosin alpha and increased annexin A1 might contribute to the apoptosis induced by h*PNAS4*.

TABLE II. Summary of Differential Proteins Identified by MALDI-Q-TOF MS

Regions on gel	Swiss-Prot accession number	Protein name	Gene name	pI/M_w	MASCOT score	2-DE	RT-PCR	Functions
1	P55072	Transitional endoplasmic reticulum ATPase	*VCP*	5.1/89321.8	136	↓	↑	Membranes transfer
2	P02545	Lamin-A/C	*LMNA*	6.6/74139.5	107	↑	↑	Formation of nuclear lamina
3	P04083	Annexin A1	*ANXA1*	6.6/38714.3	128	↑	↑	Calcium/phospholipids-binding, apoptosis
4	P40926	Malate dehydrogenase	*MDH2*	8.9/35503.3	156,78	↑	–	Metabolism
5	P30041	Peroxiredoxin-6	*PRDX6*	6.0/25035.0	233	↓	↓	Redox regulation
6	P60174	Triosephosphate isomerase	*TPI1*	6.5/26669.5	219	↓	↓	Metabolism
7	Q15056	Eukaryotic translation initiation factor 4H	*EIF4H*	6.7/27385.1	79	↓	–	Protein translation
8	P30043	Flavin reductase	*BLVRB*	7.1/22119.4	67	↓	↓	Anti-oxidation
8	P37802	Transgelin-2	*TAGLN2*	8.4/22391.5	197	↓	–	Smooth muscle contraction
9	P22392	Nucleoside diphosphate kinase B	*NME2*	8.5/17298.0	94	↓	↓	Nucleotide synthesis
10	P09382	Galectin-1	*LGALS1*	5.3/14715.7	71	↓	–	Cell differentiation
11	P06454	Prothymosin alpha	*PTMA*	3.7/12203.0	42	↓	↓	Immune, apoptosis
11	P05387	60S acidic ribosomal protein P2	*RPLP2*	4.4/11664.9	156	↓	↓	Protein synthesis
12	P30626	Sorcin	*SRI*	5.3/21676.4	40	↓	–	Drug-resistance, calcium-binding
13	P28072	Proteasome subunit beta type-6	*PSMB6*	4.8/25357.7	46	↑	↑	Proteolysis
13	P08670	Vimentin	*VIM*	5.1/53651.7	113,109	↑	–	Skeleton, apoptosis
14	O43852	Calumenin	*CALU*	4.5/37106.8	42	↓	–	Carboxylation, biding calcium
15	Q15293	Reticulocalbin-1	*RCN1*	4.9/38890.0	98	↓	↓	Biding calcium
16	Q13347	Eukaryotic translation initiation factor 3 subunit 2	*EIF3S2*	5.4/36501.9	41	↓	–	Protein translation
16	P07195	L-lactate dehydrogenase B chain	*LDHB*	5.7/36638.5	67	↓	↓	Metabolism

Malate dehydrogenase and Vimentin have two spots on the 2-DE gel, respectively.
The symbols "↓," "↑," and"–" mean up-, down-, and nonregulation in hPNAS4-induced apoptosis, respectively.

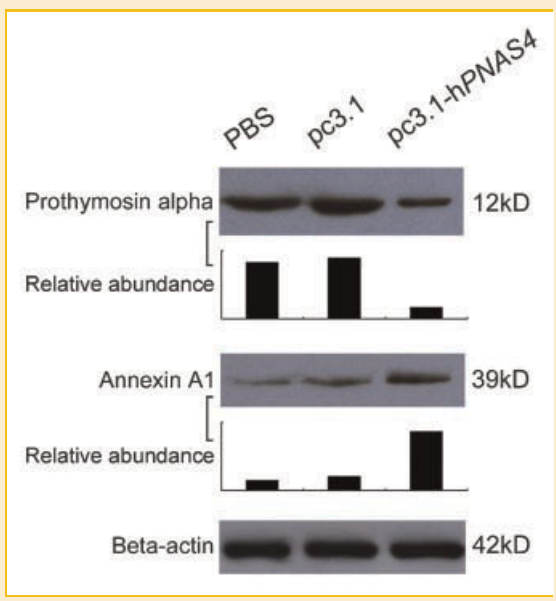

Fig. 5. Detection of prothymosin alpha and annexin A1 by Western blot. Cells were treated with PBS, pc3.1, and pc3.1-h*PNAS4*, respectively, for 48 h. Proteins were extracted and separated by 12% SDS–PAGE. Proteins were probed with primary antibodies (anti-prothymosin alpha and anti-annexin A1) and secondary antibodies conjugated with horseradish peroxidase. Beta-actin was used as equal loading control. The relative abundance of corrected band-density according to beta-actin is represented below. [Color figure can be viewed in the online issue, which is available at www.interscience.wiley.com.]

It is noticed that on 2-DE gel, two spots with lower molecular weight (less than 35 kD) were identified as vimentin that is an intermediate filament protein with molecular weight of 53.5-kD. Recent studies demonstrated vimentin is an important substrate of multiple caspases and can be cleaved by caspases 3, 6, 7, and 8 at aspartic acid site [Prasad et al., 1998; Morishima, 1999]. Hence, the cleavage of vimentin usually typifies apoptotic cell death [Müller et al., 2001; Lavastre et al., 2002]. In fact, our previous study demonstrated there was activation of caspase-3 in h*PNAS4*-induced apoptosis [Yan et al., 2009]. Therefore, we speculate the low molecular weight vimentins that appeared on 2-DE gel in this study should be cleavage products of original vimentin precursor, and we also believed the cleavage products could promote and amplify h*PNAS4*-induced apoptosis through its dismantling intermediate filaments caused by caspases activation [Hashimoto et al., 1998; Byun et al., 2001].

In summary, we investigated the changes of protein-expressing profile in h*PNAS4*-induced apoptosis applying proteomics strategy consisting of 2-DE coupled with MALDI-Q-TOF mass spectrometry. The identified differential proteins provide initial information to mechanism comprehension and functional presentation about h*PNAS4*. The transcription analyses of the differential proteins indicate that there should be post-transcription regulations that give rise to the differential protein expression. Two apoptosis-associated proteins prothymosin alpha and annexin A1 were confirmed by Western blot, and their important apoptosis-related functions could be contributed to the h*PNAS4*-induced apoptosis. The investigations on the potential interactions between h*PNAS4* and those identified differential proteins should further reveal the unknown biological function of h*PNAS4*.

REFERENCES

Bensalem N, Ventura AP, Vallée B, Lipecka J, Tondelier D, Davezac N, Dos Santos A, Perretti M, Fajac A, Sermet-Gaudelus I, Renouil M, Lesure JF, Halgand F, Laprévote O, Edelman A. 2005. Down-regulation of the anti-inflammatory protein annexin A1 in cystic fibrosis knock-out mice and patients. Mol Cell Proteomics 4:1591–1601.

Best CJ, Gillespie JW, Yi Y, Chandramouli GV, Perlmutter MA, Gathright Y, Erickson HS, Georgevich L, Tangrea MA, Duray PH, González S, Velasco A, Linehan WM, Matusik RJ, Price DK, Figg WD, Emmert-Buck MR, Chuaqui RF. 2005. Molecular alterations in primary prostate cancer after androgen ablation therapy. Clin Cancer Res 11:6823–6834.

Beyer A, Hollunder J, Nasheuer HP, Wilhelm T. 2004. Post-transcriptional expression regulation in the yeast Saccharomyces cerevisiae on a genomic scale. Mol Cell Proteomics 3:1083–1092.

Bruneel A, Labas V, Mailloux A, Sharma S, Royer N, Vinh J, Pernet P, Vaubourdolle M, Baudin B. 2005. Proteomics of human umbilical vein endothelial cells applied to etoposide-induced apoptosis. Proteomics 5: 3876–3884.

Byun Y, Chen F, Chang R, Trivedi M, Green KJ, Cryns VL. 2001. Caspase cleavage of vimentin disrupts intermediate filaments and promotes apoptosis. Cell Death Differ 8:443–450.

Chen G, Gharib TG, Huang CC, Taylor JM, Misek DE, Kardia SL, Giordano TJ, Iannettoni MD, Orringer MB, Hanash SM, Beer DG. 2002. Discordant protein and mRNA expression in lung adenocarcinomas. Mol Cell Proteomics 1:304–313.

Chen Y, Zheng W, Li Y, Zhong J, Ji J, Shen P. 2008. Apoptosis induced by methylene-blue-mediated photodynamic therapy in melanomas and the involvement of mitochondrial dysfunction revealed by proteomics. Cancer Sci 99:2019–2027.

Courcelle J, Donaldson JR, Chow KH, Courcelle CT. 2003. DNA damage-induced replication fork regression and processing in Escherichia coli. Science 299:1064–1067.

Debret R, El Btaouri H, Duca L, Rahman I, Radke S, Haye B, Sallenave JM, Antonicelli F. 2003. Annexin A1 processing is associated with caspase-dependent apoptosis in BZR cells. FEBS Lett 546:195–202.

Dong H, Ying T, Li T, Cao T, Wang J, Yuan J, Feng E, Han B, Hua F, Yang Y, Yuan J, Wang H, Xu C. 2006. Comparative proteomic analysis of apoptosis induced by sodium selenite in human acute promyelocytic leukemia NB4 cells. J Cell Biochem 98:1495–1506.

Forrest MS, Lan Q, Hubbard AE, Zhang L, Vermeulen R, Zhao X, Li G, Wu YY, Shen M, Yin S, Chanock SJ, Rothman N, Smith MT. 2005. Discovery of novel biomarkers by microarray analysis of peripheral blood mononuclear cell gene expression in benzene-exposed workers. Environ Health Perspect 113: 801–807.

Hashimoto M, Inoue S, Ogawa S, Conrad C, Muramatsu M, Shackelford D, Masliah E. 1998. Rapid fragmentation of vimentin in human skin fibroblasts exposed to tamoxifen: A possible involvement of caspase-3. Biochem Biophys Res Commun 247:401–406.

Jiang X, Kim HE, Shu H, Zhao Y, Zhang H, Kofron J, Donnelly J, Burns D, Ng SC, Rosenberg S, Wang X. 2003. Distinctive roles of PHAP proteins and prothymosin-alpha in a death regulatory pathway. Science 299:223–226.

Kim DW, Chae JI, Kim JY, Pak JH, Koo DB, Bahk YY, Seo SB. 2009. Proteomic analysis of apoptosis related proteins regulated by proto-oncogene protein DEK. J Cell Biochem 106:1048–1059.

Kurland CG. 1991. Codon bias and gene expression. FEBS Lett 285:165–169.

Lavastre V, Pelletier M, Saller R, Hostanska K, Girard D. 2002. Mechanisms involved in spontaneous and Viscum album agglutinin-I-induced human neutrophil apoptosis: Viscum album agglutinin-I accelerates the loss of antiapoptotic Mcl-1 expression and the degradation of cytoskeletal paxillin and vimentin proteins via caspases. J Immunol 168:1419–1427.

Lee KA, Shim JH, Kho CW, Park SG, Park BC, Kim JW, Lim JS, Choe YK, Paik SG, Yoon DY. 2004. Protein profiling and identification of modulators regulated by the E7 oncogene in the C33A cell line by proteomics and genomics. Proteomics 4:839–848.

Malicet C, Giroux V, Vasseur S, Dagorn JC, Neira JL, Iovanna JL. 2006. Regulation of apoptosis by the p8/prothymosin alpha complex. Proc Natl Acad Sci USA 103:2671–2676.

Maniatis T, Tasic B. 2002. Alternative pre-mRNA splicing and proteome expansion in metazoans. Nature 418:236–243.

MGC Project Team. 2004. The status, quality, and expansion of the NIH full-length cDNA project: The Mammalian Gene Collection (MGC). Genome Res 14:2121–2127.

Morishima N. 1999. Changes in nuclear morphology during apoptosis correlate with vimentin cleavage by different caspases located either upstream or downstream of Bcl-2 action. Genes Cells 4:401–414.

Müller K, Dulku S, Hardwick SJ, Skepper JN, Mitchinson MJ. 2001. Changes in vimentin in human macrophages during apoptosis induced by oxidised low density lipoprotein. Atherosclerosis 156:133–144.

Ørntoft TF, Thykjaer T, Waldman FM, Wolf H, Celis JE. 2002. Genome-wide study of gene copy numbers, transcripts, and protein levels in pairs of non-invasive and invasive human transitional cell carcinomas. Mol Cell Proteomics 1:37–45.

Pesole G, Gissi C, Grillo G, Licciulli F, Liuni S, Saccone C. 2000. Analysis of oligonucleotide AUG start codon context in eukariotic mRNAs. Gene 261: 85–91.

Prasad SC, Thraves PJ, Kuettel MR, Srinivasarao GY, Dritschilo A, Soldatenkov VA. 1998. Apoptosis-associated proteolysis of vimentin in human prostate epithelial tumor cells. Biochem Biophys Res Commun 249:332–338.

Qiu J, Gao HQ, Li BY, Shen L. 2008. Proteomics investigation of protein expression changes in ouabain induced apoptosis in human umbilical vein endothelial cells. J Cell Biochem 104:1054–1064.

Reinders J, Lewandrowski U, Moebius J, Wagner Y, Sickmann A. 2004. Challenges in mass spectrometry-based proteomics. Proteomics 4:3686–3703.

Santin AD, Zhan F, Bignotti E, Siegel ER, Cané S, Bellone S, Palmieri M, Anfossi S, Thomas M, Burnett A, Kay HH, Roman JJ, O'Brien TJ, Tian E, Cannon MJ, Shaughnessy JJ, Pecorelli S. 2005. Gene expression profiles of primary HPV16- and HPV18-infected early stage cervical cancers and normal cervical epithelium: Identification of novel candidate molecular markers for cervical cancer diagnosis and therapy. Virology 331:269–291.

Tsai IC, Hsieh YJ, Lyu PC, Yu JS. 2005. Anti-phosphopeptide antibody, P-STM as a novel tool for detecting mitotic phosphoproteins: Identification of lamins A and C as two major targets. J Cell Biochem 94:967–981.

Varshavsky A. 2003. The N-end rule and regulation of apoptosis. Nat Cell Biol 5:373–376.

Wittmann-Liebold B, Graack HR, Pohl T. 2006. Two-dimensional gel electrophoresis as tool for proteomics studies in combination with protein identification by mass spectrometry. Proteomics 6:4688–4703.

Yan F, Gou L, Yang J, Chen L, Tong A, Tang M, Yuan Z, Yao S, Zhang P, Wei Y. 2009. A novel pro-apoptosis gene PNAS4 that induces apoptosis in A549 human lung adenocarcinoma cells and inhibits tumor growth in mice. Biochimie 91:502–507.

Yao S, Xie L, Qian M, Yang H, Zhou L, Zhou Q, Yan F, Gou L, Wei Y, Zhao X, Mo X. 2008. Pnas4 is a novel regulator for convergence and extension during vertebrate gastrulation. FEBS Lett 582:2325–2332.

Zhao B, Poh CL. 2008. Insights into environmental bioremediation by microorganisms through functional genomics and proteomics. Proteomics 8:874–881.

Zong Q, Schummer M, Hood L, Morris DR. 1999. Messenger RNA translation state: The second dimension of high-throughput expression screening. Proc Natl Acad Sci USA 96:10632–10636.